ESRF	**Experiment title:** Forming osteocytes mapped by 50 nm voxel size fluorescence/diffraction tomography	**Experiment number**: LS-2798
Beamline:	**Date of experiment**: from: 04-04-2018 to: 08-04-2018	**Date of report**: 20-02-2020
Shifts:	**Local contact(s)**: Tilman Grünewald and Manfred Burghammer	*Received at ESRF:*

Names and affiliations of applicants (* indicates experimentalists):

Henrik Birkedal, Aarhus University, Denmark

Nina Kølln Wittig, Aarhus University, Denmark

Jonas Palle, Aarhus University, Denmark

Maria Francesca di Filippo, Aarhus University, Denmark

Report:

Summary

The aim of the experiment was to investigate the structure and composition of the bone associated with the lacuno-canalicular network (LCN) around mature and forming osteocytes by combined fluorescence and diffraction computed tomography with 50 nm voxel size. We succeeded in collecting a full tomographic data set and several 2D projections with a sub-50 nm X-ray beam. Due to beam damage and loss of a sample we were unable to tomographically reconstruct all desired data. Nonetheless, we recorded a large amount of 50 nm resolution 2D scans of fluorescence and diffraction from LCN-associated bone allowing for a detailed investigation of the element composition and mineral properties of this bone.

Scientific aim of the experiment

The LCN consists of osteocytes embedded in lacunae connected by canaliculi and occupies a large percentage of human bone. The LCN is important for the bone biology affecting both the mechanical properties of bone and the cellular processes inside the bone.[1-2] In addition the LCN is believed to have an important role in mechanosensing and remodeling of bone[3]. Despite the importance of the LCN, the influence of the LCN on the surrounding bone matrix is poorly understood. The aim of the experiment was to investigate the structure and composition of the LCN-associated bone around mature and forming osteocytes. This, we aimed to do using combined fluorescence and diffraction computed tomography with a 50 nm voxel size. The X-ray fluorescence (XRF) information will reveal the distribution of oligo-elements, such as Zn, in the bone and the X-ray diffraction will give insight into the crystallographic properties of the bone mineral surrounding the LCN. We have previously performed a technically similar experiment under proposal code LS-2654 that demonstrated the feasibility of the experiment.

Samples and Setup

Samples: Samples were produced from human bone from patients suffering from hypoparathyroidism. These patients are unable to form new bone due to lack of PTH, an important hormone facilitating bone formation. The patients were treated with recombinant PTH that restarts bone formation. This medicinal control of bone formation allows us to distinguish between old and newly formed bone.

For the tomographic experiment a rod-shaped sample was produced using focused ion beam (FIB) milling, from an area adjacent to an osteocyte in newly formed bone (Figure 1). A second sample was produced in a similar fashion from an area adjacent to an old osteocyte, but unfortunately this sample broke during transport to the ESRF.

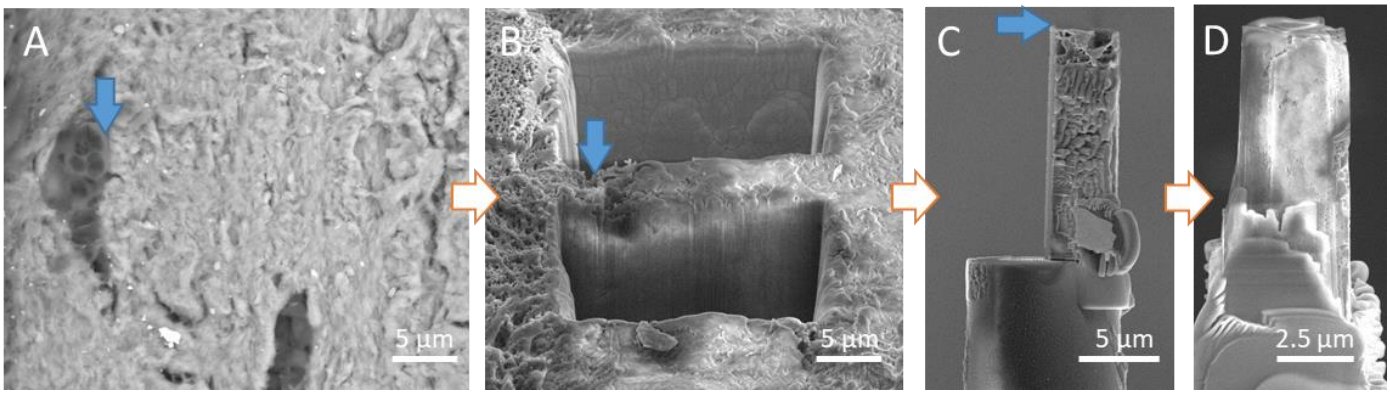

Figure 1. SEM images at different stages of the sample preparation. An osteocyte was chosen based on a back-scattered electron micrograph (A) and deep holes were etched next to the sample (B) in order to be able to cut it free with the FIB. Sample was cut free, lifted out and placed on top a glass needle (C). Finally, corners were trimmed so the sample became octagonal (D). Scale bars are 5 µm in image A, B, C and 2.5 µm in D.

A number of backup samples for 2D scanning were produced as well. Bone slices of ~30 µm thickness were manufactured using a diamond saw and abrasive paper from bone from the same patient as above.

Setup: The experimental setup was implemented and improved based on previous experience from experiment LS-2654. We used the MLL lenses developed by Kubec, Niese, Keckes et al.[4], to focus a 12.7 keV x-ray beam to a spot size of 42×48 nm^2 (horizontal×vertical) with a flux of ~5×10^{10} photons/s – four times higher than in the previous experiment. The sample was raster scanned in a 50×50 nm^2 raster scanning pattern from 91 different projection angles at 2° intervals. For each point in the raster pattern a diffraction signal was recorded using the Eiger4M detector and the fluorescence signal was recorded using a Vortex EM fluorescence detector, using an exposure time of 100 ms – twice that of the previous experiment in order to get better count statistics.

Preliminary findings

Based on the fluorescence and diffraction signal of the first projections the experiment was very promising. We show that both fluorescence and diffraction can be detected from a sample only 3 µm thick using a 100 ms exposure time. Projection images of the calcium fluorescence intensity show the outline of the sample (Figure 2, left). These projections show the measured intensity as recorded and thus suffer from shaky edges and shifted lines due to the instability of motor position. At 50 nm resolution the sample will move a bit between line scans, despite our best efforts to implement instability-reducing measures, such as turning off all motors except for the scanning piezo motors. The shift in position between lines in the scan will be corrected for by aligning each line in the image using our own alignment software.

When comparing the calcium XRF map to the zinc XRF map (Figure 2, right) it can be seen that in an area of low Ca concentration a higher Zn concentration is present. Zn is known to play an important role in the formation of bone, and can often be found in higher concentration in the canaliculi connecting bone osteocytes.[5] As the sample is taken from an area near an osteocyte we are convinced that the signal originates from canaliculi.

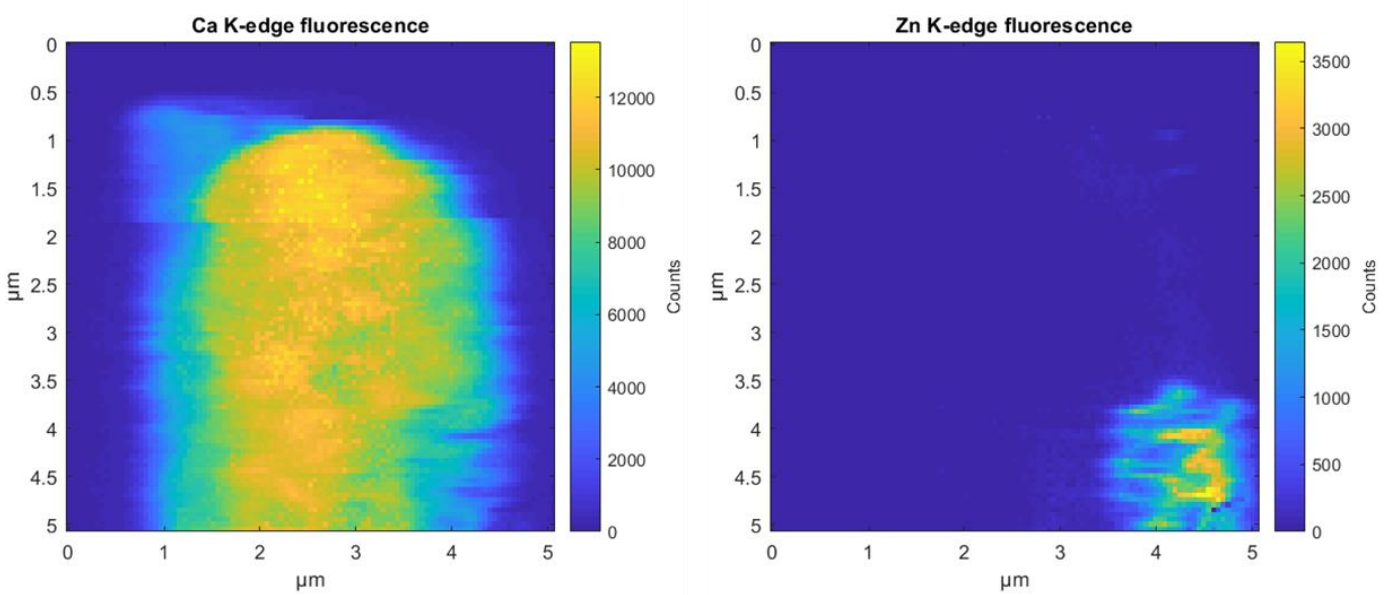

Figure 2. Projection images of the calcium and zinc fluorescence intensity from one of the first projections in the tomographic data set.

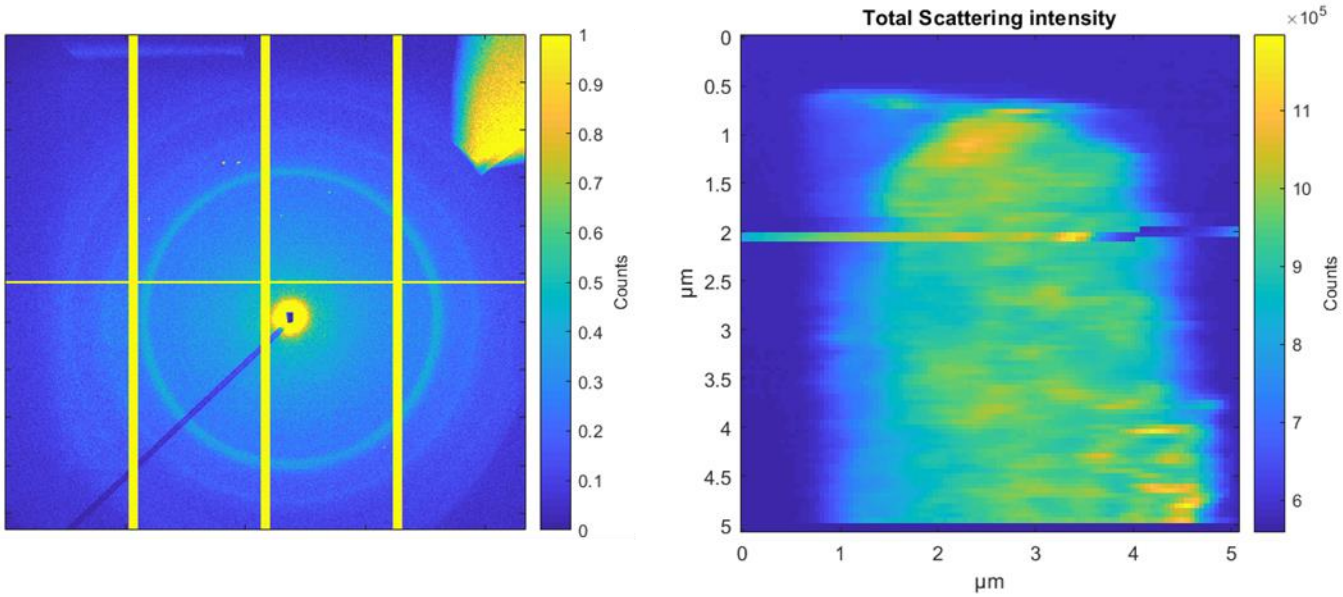

Figure 3. An average diffractogram meaned over 200 different point on the sample is shown to the left. On the right is an image of the total scattering intensity from the same projection angle as seen in figure 2. Each pixel in the image has a value corresponding to the sum of the scattered x-ray intensity.

Despite the promising results in the first approximately 40 projections the sample started to take critical damage from the x-ray exposure and by the final projection angle it had completely changed its shape. For this reason tomographical reconstruction of this dataset is not possible, and all further analysis will be based on the projection images. Additionally were were able to conduct 2D scanning experiments on ~30 µm thin bone slices from the same type of bone recording flouorescence and diffraction. These data allowed mapping the mineralization front and appear to provide excellent insights into bone formation.

Conclusion and further proceedings

We managed to collect a good dataset consisting of a range of 2D projection images of fluorescence and diffraction with 50 nm theoretical resolution.

We anticipate that these data will be part of two publications. For the small sample meant for tomography we expect to publish a case study of the LCN-associated bone matrix. The data from the slices of bone will be incorporated in a broader study of the mineralization process in human bone, based on PTH bone.

References

1. Reznikov, N.; Shahar, R.; Weiner, S., Bone hierarchical structure in three dimensions. *Acta Biomaterialia* **2014,** *10* (9), 3815-3826.
2. Wittig, N. K.; Palle, J.; Østergaard, M.; Frølich, S.; Birkbak, M. E.; Spiers, K. M.; Garrevoet, J.; Birkedal, H., Bone Biomineral Properties Vary across Human Osteonal Bone. *ACS Nano* **2019**.
3. Webster, D. J.; Schneider, P.; Dallas, S. L.; Müller, R., Studying osteocytes within their environment. *Bone* **2013,** *54* (2), 285-295.
4. Kubec, A.; Melzer, K.; Gluch, J.; Niese, S.; Braun, S.; Patommel, J.; Burghammer, M.; Leson, A., Point focusing with flat and wedged crossed multilayer Laue lenses. *Journal of Synchrotron Radiation* **2017,** *24* (2), 413-421.
5. Yamaguchi, M., Role of zinc in bone formation and bone resorption. *The Journal of Trace Elements in Experimental Medicine* **1998,** *11* (2-3), 119-135.